

Pilot Distributions for Phase Noise Estimation in Electro-Optic Frequency Comb Systems

Mohammad Farsi⁽¹⁾, Magnus Karlsson⁽²⁾, and Erik Agrell⁽¹⁾

⁽¹⁾ Dept. of Electrical Engineering, Chalmers Univ. of Technology, Sweden, farsim@chalmers.se

⁽²⁾ Dept. of Microtechnology and Nanoscience, Chalmers Univ. of Technology, Sweden

Abstract We explore the optimal pilot positioning for phase tracking in electro-optic frequency comb setups. We show that, in contrast to previous results for regular multichannel systems, allocating the first and the last channels for pilots is optimal given a fixed pilot overhead. ©2023 The Author(s)

Introduction

Resource sharing among multiple wavelength channels is necessary for co-integrating multiple optical transceivers without exceeding power and heat constraints. The electro-optic frequency comb (EO comb), serving as a multi-wavelength source, provides uniformly spaced carriers for spectral superchannels, enabling co-integration. Moreover, they have applications in metrology, sensing, and telecommunications.

The phase noise (PN) among different comb lines is fully correlated as a result of sharing the same light source. This enables potential resource savings by utilizing joint phase estimation. This becomes more important with high-order modulation formats where PN is more detrimental.

The inherent PN correlation between optical comb lines can reduce the computational complexity in digital signal processing through optical comb regeneration techniques^[1] or improve the performance of pilot-aided tracking schemes such as reference-assisted (RA) (also known as master–slave) processing^{[2],[3]} or joint-channel processing^[4]. Previous studies have shown that distributing pilots in time and channel in a grid fashion works best for multichannel systems^[5]. In^{[6],[7]} it was shown that the optimal pilot placement for space-division multiplexing systems depends on the amount of PN correlation across channels. However, there has been no investigation of pilot placement in the context of EO comb systems where the channels are fully correlated.

In this paper, we explore the use of phase correlation in phase tracking in EO combs and analyze pilot placement methods. Optimal pilot positioning is studied and unlike a regular multichannel system, the outer comb lines are found to be optimal for certain estimators. The pilot distribution can substantially impact the bit error rate, with a potential for significant improvement.

System Model

Consider uncoded single-polarization transmission in L wavelength-division multiplexing (WDM)

channels generated by an EO comb. Also, assume negligible (or already compensated) impairments with the exception of PN and amplified spontaneous emission noise. For EO combs, most of the PNs originate from the continuous wave (CW) laser and the radio frequency (RF) oscillator, which are shared between all comb lines, resulting in correlated PNs across the channels^[8].

The transmitted symbol block in each channel is a random vector of length N , where each element is drawn uniformly from a set of equiprobable constellation points. Pilots, with known values and locations, are inserted. The resulting discrete-time baseband EO comb channel model at time $k \in \{1, 2, \dots, N\}$ and channel index $m \in \{-M, \dots, M\}$ where $M = (L + 1)/2$ and L is the number of channels and odd, is

$$\mathbf{y}_{m,k} = e^{j\theta_{m,k}} (\mathbf{x}_{m,k} + \mathbf{z}_{m,k}), \quad (1)$$

where $\mathbf{y}_{m,k}$, $\mathbf{x}_{m,k}$, $\theta_{m,k}$, and $\mathbf{z}_{m,k}$ are the received samples, transmitted symbols, total PN, and additive, zero-mean, complex, identically and independently distributed (i.i.d.) Gaussian noise, respectively. Here,

$$\theta_{m,k} = \theta_k^c + m\theta_k^r, \quad (2)$$

where θ_k^c and θ_k^r denote the PNs induced by the CW laser and RF oscillator, respectively. The PN sources are statistically independent of each other and all the other random variables and are defined¹ as Gaussian random walks^{[8],[9]}

$$\theta_k^{c/r} = \theta_{k-1}^{c/r} + \Delta_k^{c/r}, \quad (3)$$

where $\theta_0^{c/r}$ are uniformly distributed in the interval $[-\pi, \pi)$. Moreover, $\Delta_k^{c/r}$ are independent zero-mean Gaussian variables with variances $\sigma_{c/r}^2 = 2\pi\Delta\nu^{c/r}T_s$. These variances describe the drift speed of their corresponding PN. Here, T_s is the symbol duration and $\Delta\nu^c$ (typically 1 – 100 kHz) and $\Delta\nu^r$ (typically 1 – 1000 Hz) denote the CW

¹The c/r convention is to avoid redundant repetitions.

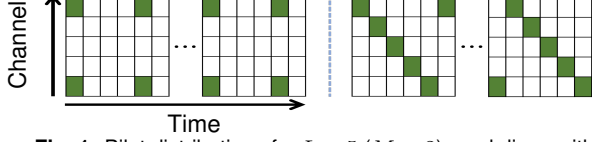


Fig. 1: Pilot distributions for $L = 5$ ($M = 2$) comb lines with $\alpha_p = 1/5$: RAD (left) and WDD (right), with dark and white blocks representing pilots and data symbols, respectively.

laser and RF oscillator linewidths, respectively.

Defining $\underline{\theta}_k = (\theta_{1,k}, \dots, \theta_{M,k})$, we can write the PN innovation vector $\underline{\theta}_k = \mathbf{T} \cdot [\theta_k^c, \theta_k^r]^T$, where \mathbf{T} is a $2 \times L$ mixing matrix

$$\mathbf{T} = \begin{bmatrix} 1 & -M \\ \vdots & \vdots \\ 1 & M \end{bmatrix}. \quad (4)$$

Reference-Assisted Phase Tracking Scheme

The RA strategy designates $2 \leq D \leq L$ channels as *reference* channels, where phase tracking is performed and estimated phases are used to correct the PN of all the remaining channels, which are designated as *assisted*.

Let $\mathcal{D} = \{d_1, \dots, d_D\}$ be a set with distinct elements denoting the reference channel indices. Clearly, all the members of \mathcal{D} are integers in the range $[-M, M]$. The $D \times 1$ PN vector of the reference channels can be written as $\underline{\theta}_k^{\mathcal{D}} = \mathbf{Q} \cdot [\theta_k^c, \theta_k^r]^T$, where

$$\mathbf{Q} = \begin{bmatrix} 1 & d_1 \\ \vdots & \vdots \\ 1 & d_D \end{bmatrix}. \quad (5)$$

Note that we can write $\underline{\theta}_k = \mathbf{T}\mathbf{Q}^\dagger \underline{\theta}_k^{\mathcal{D}}$, where $\mathbf{Q}^\dagger = (\mathbf{Q}^T \mathbf{Q})^{-1} \mathbf{Q}^T$ is the Moore–Penrose inverse of \mathbf{Q} .

Without loss of generality, for the reference channels, we define the $D \times 1$ estimated phase vector $\hat{\underline{\theta}}_k^{\mathcal{D}}$ as

$$\hat{\underline{\theta}}_k^{\mathcal{D}} = \underline{\theta}_k^{\mathcal{D}} + \underline{\mathbf{w}}_k^{\mathcal{D}}, \quad (6)$$

where $\underline{\mathbf{w}}_k^{\mathcal{D}}$ is the $D \times 1$ estimation error vector. Its distribution depends on the utilized phase estimation algorithm which is left free to choose. To apply the estimated phases to the assisted channels, we need to form the $L \times 1$ vector of estimated phases as $\hat{\underline{\theta}}_k = \mathbf{T}\mathbf{Q}^\dagger \hat{\underline{\theta}}_k^{\mathcal{D}}$, which gives

$$\hat{\underline{\theta}}_k = \underline{\theta}_k + \mathbf{T}\mathbf{Q}^\dagger \underline{\mathbf{w}}_k^{\mathcal{D}}. \quad (7)$$

Pilot Placement for RA Phase Tracking

The optimal reference channel index set \mathcal{D}^* is the solution to

$$\mathcal{D}^* = \arg \min_{\mathcal{D}} \mathbb{E} \left[\left\| \underline{\theta}_k - \hat{\underline{\theta}}_k \right\|^2 \right], \quad (8)$$

where $\hat{\underline{\theta}}_k$ is the $L \times 1$ estimated innovation vector in (7), which is obtained from the reference channels. Substituting (7) into (8), we obtain

$$\mathcal{D}^* = \arg \min_{\mathcal{D}} \mathbb{E} \left[\left\| \mathbf{T}\mathbf{Q}^\dagger \underline{\mathbf{w}}_k^{\mathcal{D}} \right\|^2 \right]. \quad (9)$$

Note that the solution of (9) is applicable to any estimation algorithm used on the reference channels. For instance, if an unbiased estimator is selected such that the elements of $\underline{\mathbf{w}}_k^{\mathcal{D}}$ become i.i.d. and independent of \mathcal{D} , the optimal solution becomes independent of the estimator and can be computed as $\mathcal{D}^* = \arg \min_{\mathcal{D}} \left\| \mathbf{T}\mathbf{Q}^\dagger \right\|_{\text{F}}^2$, where $\|\cdot\|_{\text{F}}^2$ denotes the Frobenius norm. It can be shown that the optimal set can be formulated as

$$\mathcal{D}^* = \left\{ -M, -M+1, \dots, -M + \lfloor (D+1)/2 \rfloor, \right. \\ \left. M+1 - \lfloor D/2 \rfloor, \dots, M-1, M \right\}. \quad (10)$$

Pilot Distributions

The estimation technique can be done using either an RA or a joint-channel processing scheme, depending on the pilot distribution. Let $\alpha_p \in [0, 1]$ represent the average rate across all channels.

Two pilot distributions for joint-channel processing were examined: reference-assisted distribution (RAD), in which pilots are positioned at the same time index across a group of reference channels identified by \mathcal{D} , and wrapped diagonal distribution (WDD), which places pilots along the diagonal in a wrapped pattern. In RAD, pilots are only located in the channels specified by \mathcal{D} , while in WDD, pilots are distributed across all channels using the wrapped diagonal approach. The pilot rate α_p determines the time spacing between the pilots for both distribution types. Fig. 1 depicts examples of the distributions. Moreover, the pilot rate of RAD is restricted to $\alpha_p \leq D/L$ and for WDD it is limited to $\alpha_p \leq 1/L$.

Simulation Setup

Monte Carlo simulations of uncoded 64-ary quadrature-amplitude modulation (QAM) at a symbol rate of $R_s = 20$ Gbaud, using system model (1), were performed with $N = 10^5$ symbols per channel. The number of channels L was varied between 11 to 101, with a fixed $\alpha_p = 1\%$ pilot overhead and a signal-to-noise-ratio yielding a bit error rate (BER) of 10^{-3} for PN-free transmission. The CW laser linewidth was fixed at $\Delta\nu^c = 100$ kHz while the RF oscillator linewidth was varied within the practical range of $\Delta\nu^r \in [1, 10^4]$ Hz. The extended Kalman smoother algorithm from^[10] was used for phase tracking due to its adaptability to various pilot distributions. For any set of reference channels \mathcal{D} , we define the mean estimation error $\mathcal{E}^{\mathcal{D}} = \mathbb{E}[\|\mathbf{T}\mathbf{Q}^\dagger \underline{\mathbf{w}}_k^{\mathcal{D}}\|^2]$.

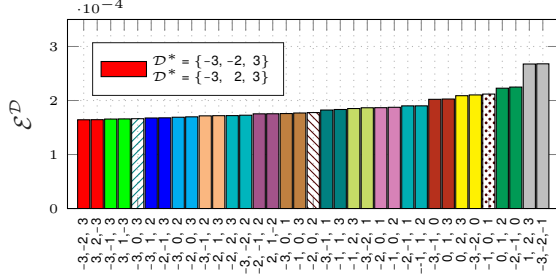
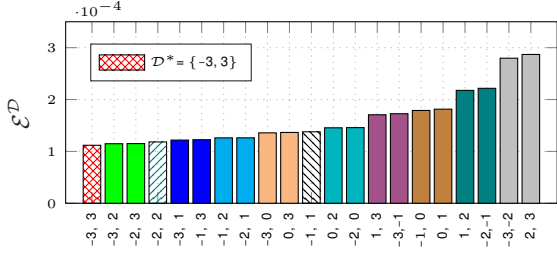


Fig. 2: The mean estimation error \mathcal{E}^D for all possible selections of $D = 2$ (left) and $D = 3$ (right) reference channels when $L = 7$ ($M = 3$) and $\alpha_p = 1/7$. The horizontal axis shows the selected reference channels \mathcal{D} .

Fig. 2 illustrates the mean estimation error \mathcal{E}^D for all possible choices of reference channels for $D = 2$ (left) and $D = 3$ (right) when $L = 7$ ($M = 3$) and $\alpha_p = 1/7$. The color-coded bars in the figure indicate channel symmetry, with bars of the same color having identical estimation errors and uniquely hashed bars having no identical twin bars. Small variations in estimation errors are due to randomness. In both cases, the optimal reference channel set indicated by hashed red (left) and solid red (right) aligns with (10). Interestingly, for $D = 3$, the best channel set is not the uniform choice of channels (first, middle, and last), but rather $\mathcal{D}^* = \{-3, -2, 3\}$ or its mirror image $\mathcal{D}^* = \{-3, 2, 3\}$. The optimal set of two reference channels $\mathcal{D}^* = \{-3, 3\}$ results in slightly better \mathcal{E}^D than the case with three reference channels $\mathcal{D}^* = \{-3, -2, 3\}$.

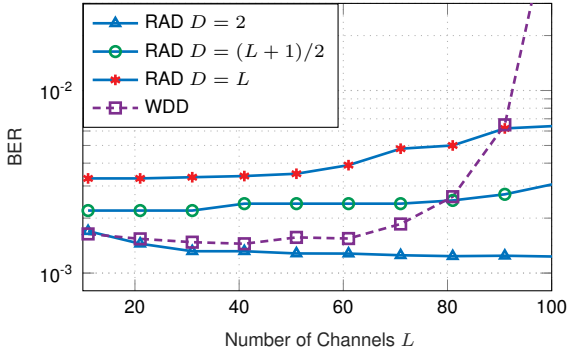


Fig. 3: BER of various pilot distribution for a fixed pilot rate $\alpha_p = 1\%$ versus the number of channels L . The RF oscillator linewidth is $\Delta\nu^r = 100\text{Hz}$.

Fig. 3 shows the BER as a function of L for different pilot distributions at a fixed pilot rate of $\alpha_p = 1\%$ and RF oscillator linewidth of $\Delta\nu^r = 100\text{Hz}$. For each D and L , the reference channels are optimally selected according to (10). Our findings suggest that the best RAD is achieved when $D = 2$ reference channels are used (i.e., $\mathcal{D} = \{-M, M\}$), while the poorest performance is observed when pilots are placed in all channels (i.e., $\mathcal{D} = \{-M, -M+1, \dots, M\}$). Additionally, it is observed that increasing the number of reference channels D leads to higher BER, suggesting that $D = 2$ is optimal at a fixed pilot rate. For $L > 40$, the PN of the RF oscillator becomes more significant at the outer channels, leading to faster phase changes. This makes it harder to ac-

curately estimate the phase in the outer channels using the inner channels, which may explain why WDD performs poorly at higher values of L .

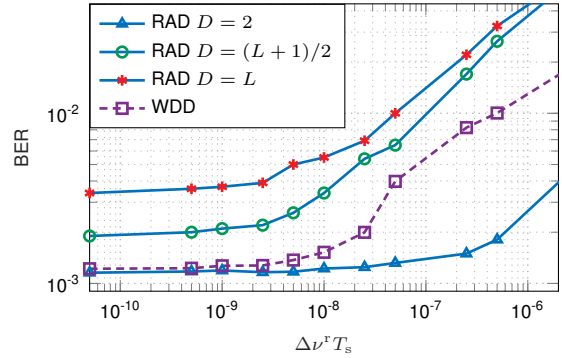


Fig. 4: BER of different pilot distribution types is shown for a fixed pilot rate $\alpha_p = 1\%$ and $\Delta\nu^c = 100\text{kHz}$.

Fig. 4 depicts the BER versus normalized RF oscillator linewidth $\Delta\nu^r T_s$ for $L = 51$ comb lines using $\alpha_p = 1\%$. Again, for each D , the set of reference channels are chosen according to (10). For $\Delta\nu^r T_s \leq 10^{-8}$, WDD and RAD with $D = 2$ perform similarly, but RAD with $D = 2$ outperforms the other pilot distributions at higher values of $\Delta\nu^r T_s$. Furthermore, it is evident that the optimal performance is achieved when $D = 2$ reference channels are utilized, as it outperforms the other values across the range of studied $\Delta\nu^r T_s$.

Our hypothesis is that when there are time slots available to fill with pilots (i.e., $\alpha_p \leq 2/L$), the optimal number of reference channels is 2 ($D = 2$). Following the same logic, we speculate that $D_{opt} = \max\{2, \lceil \alpha_p L \rceil\}$.

Conclusion

Several types of pilot distributions were compared through Monte Carlo simulations in terms of the resulting BER performance for tracking correlated PN in EO comb systems. It was shown theoretically and confirmed by simulations that for certain phase estimators, the optimal reference channels are the outer channels (first and last), contrary to regular WDM channels where pilots are placed in all channels.

Acknowledgements: This work was supported by the Knut and Alice Wallenberg Foundation, grant No. 2018.0090.

References

- [1] B. J. Puttnam, J. Sakaguchi, J. M. D. Mendinueta, *et al.*, "Investigating self-homodyne coherent detection in a 19 channel space-division-multiplexed transmission link", *Optics Express*, vol. 21, no. 2, pp. 1561–1566, 2013.
- [2] M. D. Feuer, L. E. Nelson, X. Zhou, *et al.*, "Joint digital signal processing receivers for spatial superchannels", *IEEE Photonics Technology Letters*, vol. 24, no. 21, pp. 1957–1960, 2012.
- [3] L. Lundberg, M. Mazur, A. Lorences-Riesgo, M. Karlsson, and P. A. Andrekson, "Joint carrier recovery for DSP complexity reduction in frequency comb-based superchannel transceivers", in *European Conference on Optical Communication (ECOC)*, IEEE, 2017, Th.1.D.3.
- [4] A. F. Alfredsson, E. Agrell, H. Wymeersch, *et al.*, "Pilot-aided joint-channel carrier-phase estimation in space-division multiplexed multicore fiber transmission", *Journal of Lightwave Technology*, vol. 37, no. 4, pp. 1133–1142, 2018.
- [5] A. F. Alfredsson, E. Agrell, M. Karlsson, and H. Wymeersch, "Pilot distributions for joint-channel carrier-phase estimation in multichannel optical communications", *Journal of Lightwave Technology*, vol. 38, no. 17, pp. 4656–4663, 2020.
- [6] A. F. Alfredsson, E. Agrell, H. Wymeersch, and M. Karlsson, "Pilot distributions for phase tracking in space-division multiplexed systems", in *European Conference on Optical Communication (ECOC)*, IEEE, 2017, P1.SC3.48.
- [7] E. Agrell, A. Alfredsson, B. J. Puttnam, R. S. Luís, G. Rademacher, and M. Karlsson, "Modulation and detection for multicore superchannels with correlated phase noise", in *CLEO: Science and Innovations*, Optica Publishing Group, 2018, SM4C–3.
- [8] L. Lundberg, M. Karlsson, A. Lorences-Riesgo, *et al.*, "Frequency comb-based WDM transmission systems enabling joint signal processing", *Applied Sciences*, vol. 8, no. 5, p. 718, 2018.
- [9] A. Ishizawa, T. Nishikawa, A. Mizutori, *et al.*, "Phase-noise characteristics of a 25-GHz-spaced optical frequency comb based on a phase-and intensity-modulated laser", *Optics express*, vol. 21, no. 24, pp. 29 186–29 194, 2013.
- [10] A. F. Alfredsson, E. Agrell, and H. Wymeersch, "Iterative detection and phase-noise compensation for coded multichannel optical transmission", *IEEE Transactions on Communications*, vol. 67, no. 8, pp. 5532–5543, 2019.